Adaptive optics scanning laser ophthalmoscopy

Austin Roorda, Fernando Romero-Borja, William J. Donnelly III, Hope Queener
College of Optometry, University of Houston, Houston Texas 77204-2020
aroorda@uh.edu

Thomas J. Hebert
Department of Computer and Electrical Engineering, University of Houston, Houston, TX 77204-4007

Melanie C.W. Campbell
School of Optometry, University of Waterloo, Waterloo, Ontario, Canada N2L 3G1

Abstract: We present the first scanning laser ophthalmoscope that uses adaptive optics to measure and correct the high order aberrations of the human eye. Adaptive optics increases both lateral and axial resolution, permitting axial sectioning of retinal tissue *in vivo*. The instrument is used to visualize photoreceptors, nerve fibers and flow of white blood cells in retinal capillaries.

OCIS codes: (010.1080) adaptive optics; (170.0110) imaging systems; (170.4470) ophthalmology

References and Links

1. R. H. Webb, G. W. Hughes, and O. Pomerantzeff, "Flying spot TV ophthalmoscope," Appl. Opt. **19**, 2991-2997 (1980).
2. R. H. Webb and G. W. Hughes, "Scanning laser ophthalmoscope," IEEE Transactions on Biomedical Engineering **28**, 488-492 (1981).
3. R. H. Webb, G. W. Hughes, and F. C. Delori, "Confocal scanning laser ophthalmoscope," Appl. Opt. **26**, 1492-1499 (1987).
4. J. Liang, D. R. Williams, and D. Miller, "Supernormal vision and high-resolution retinal imaging through adaptive optics," J. Opt. Soc. Am. A **14**, 2884-2892 (1997).
5. A. Roorda and D. R. Williams, "The arrangement of the three cone classes in the living human eye," Nature **397**, 520-522 (1999).
6. R. H. Webb and F. C. Delori, "How we see the retina," in *Laser Technology in Ophthalmology*, J. Marshall, ed. (Kugler & Ghedini Publications, Amsterdam, 1988). pp. 3-14.
7. W. J. Donnelly, F. Romero-Borja, and A. Roorda, "Optimal pupil size for axial resolution in the human eye," Invest. Ophthalmol. Vis. Sci. **42**, 161 (2001).
8. R. N. Weinreb and A. W. Dreher, "Reproducibility and accuracy of topographic measurements of the optic nerve head with the laser tomographic scanner," in *Laser Scanning Ophthalmoscopy and Tomography*, J. E. Nasemann and R. O. W. Burk, eds. (Quintessenz, Berlin, 1990).
9. R. Birngruber, U. Schmidt-Erfurth, S. Teschner, and J. Noack, "Confocal laser scanning fluorescence topography: a new method for three-dimensional functional imaging of vascular structures," Graefe's Arch. Clin. Exp. Ophthalmol. **238**, 559-565 (2000).
10. D. Bartsch, G. Zinser, and W. R. Freeman, "Resolution improvement in confocal scanning laser tomography of the human fundus," Vision Science and its Applications: Technical Digest (OSA, Washington, D. C.) , 134-137 (1994).
11. A. W. Dreher, J. F. Bille, and R. N. Weinreb, "Active optical depth resolution improvement of the laser tomographic scanner," Appl. Opt. **28**, 804-808 (1989).
12. S. A. Burns, S. Marcos, A. E. Elsner, and S. Bara. "Contrast improvement for confocal retinal imaging using phase correcting plates," Opt. Letters **27**, 400-402 (2002).
13. A. Roorda and M. C. W. Campbell, "Confocal scanning laser ophthalmoscope for real-time photoreceptor imaging in the human eye," Vision Science and its Applications: Technical Digest (OSA, Washington, D. C.) **1**, 90-93 (1997).
14. A. Roorda, M. C. W. Campbell, and C. Cui, "Optimal entrance beam location improves high resolution retinal imaging in the CSLO," Invest. Ophthalmol. Vis. Sci. Supplem. **38**, 1012 (1997).
15. A. R. Wade and F. W. Fitzke, "*In vivo* imaging of the human cone-photoreceptor mosaic using a confocal laser scanning ophthalmoscope," Lasers and Light in Ophthalmology **8**, 129-136 (1998).
16. A. R. Wade and F. W. Fitzke, "A fast, robust pattern recognition system for low light level image registration and its application to retinal imaging," Optics Express **3**, 190-197 (1998).
17. J. Porter, A. Guirao, I. G. Cox, and D. R. Williams, "Monochromatic aberrations of the human eye in a large population," J. Opt. Soc. Am. A **18**, 1793-1803 (2001).

#1011 - $15.00 US Received March 28, 2002; Revised April 24, 2002

18. W. J. Donnelly, "Improving Imaging in the Confocal Scanning Laser Ophthalmoscope," M.S. dissertation, (University of Houston, Houston, TX, 2001).
19. H. Hofer, P. Artal, J. L. Aragon, and D. R. Williams, "Dynamics of the eye's wave aberration," J. Opt. Soc. Am. A **18**, 497-506 (2001).
20. D. R. Williams, J. Liang, D. Miller, and A. Roorda, "Wavefront Sensing and Compensation for the Human Eye," in *Adaptive Optics Engineering Handbook*, R. K. Tyson, ed. (Marcel Dekker, New York, 1999). pp. 287-310.
21. T. Wilson and C. J. R. Sheppard, "Theory And Practice of Scanning Optical Microscopy," . (Academic Press, London, 1984).
22. A. Roorda, "Double Pass Reflections in the Human Eye," Ph.D. dissertation, (University of Waterloo, Waterloo, Canada, 1996).
23. T. Wilson, "The role of the pinhole in confocal imaging systems," in *The Handbook of Biological Confocal Microscopy*, J. B. Pawley, ed. (Plenum Press, New York, 1990). pp. 99-113.
24. Full-length uncompressed movies can be downloaded from the *Adaptive Optics Scanning Laser Ophthalmoscope Website*, http://www.opt.uh.edu/research/aroorda/aoslo.htm, (University of Houston, Houston, TX, 2002).
25. D. R. Williams, "Topography of the foveal cone mosaic in the living human eye," Vision Res. **28**, 433-454 (1988).
26. J. I. Yellot Jr, "Spectral analysis of spatial sampling by photoreceptors: Topological disorder prevents aliasing," Vision Res. **22**, 1205-1210 (1982).

1. Introduction

The invention of the scanning laser ophthalmoscope (SLO) by Webb et. al. [1, 2] represented a major advance in ophthalmoscopy. The SLO offered a new and unique imaging modality for the living human eye, conferring several advantages, which included improved efficiency in light collection and real-time imaging. One of the most important advantages was that the use of a scanning laser source and a confocal pinhole provided higher contrast images compared to conventional flood illuminated imaging systems [3]. A more recent advance in ophthalmic imaging occurred when Liang et al. used adaptive optics (AO) to compensate for monochromatic aberrations of the eye. They improved the quality of retinal images from a CCD fundus camera to the extent where it was possible to visualize [4] and measure the properties of microscopic structures, such as photoreceptors [5], in the living human eye. In this paper we present the first results from an instrument that combines the two technologies. We have constructed an Adaptive Optics Scanning Laser Ophthalmoscope (AOSLO), a SLO that uses AO, to correct high-order aberrations and provide real-time, microscopic views of the living human retina with unprecedented optical quality.

A major advantage of the SLO is its ability to optically section the retina, which is a thick, weakly scattering, multi-layered tissue [6]. However, due to the aberrations of the eye, the typical axial resolution is limited to over 200 μm [7]. Because of this limit imposed by the aberrations, the SLO is more commonly used for detection of layers, but not true axial sectioning [8, 9]. Various attempts have been made to correct these aberrations for SLO imaging. Bartsch et al. measured improvements in axial resolution after compensating the aberrations of the cornea with a rigid contact lens [10]. This method only corrected for some corneal aberrations, but did not correct the aberrations of the whole eye, which includes those of the crystalline lens. An early effort to use AO to improve tomography in a SLO was made in 1989 by Dreher et al. [11]. They used a 13-segment adjustable mirror to correct for ocular aberrations. However, at that time they did not use wavefront sensing to measure the aberrations of the eye and the mirror was limited to compensating only the measured astigmatism in the eye. They obtained moderate improvements in axial resolution. A more recent effort to correct aberrations was made by Burns et al. who used custom-built phase-correcting plates to compensate the higher order aberrations of the eye [12]. After correcting the aberrations of an individual's eye, they measured improvements in contrast of SLO images of a blood vessel of 26% and the images (3 degree field of view) revealed features not previously seen in the uncorrected images.

SLOs that do not use AO have been used for high-resolution retinal imaging. Roorda and Campbell used a custom-built SLO to image the retina over a 1.5 x 1.5 degree field near the fovea. They were able to estimate the spacing of photoreceptors through Fourier analysis

#1011 - $15.00 US Received March 28, 2002; Revised April 24, 2002

of multiple frames, but were unable to resolve the contiguous photoreceptor mosaic [13]. They also found that image quality could be improved by locating the entrance pupil in the least aberrated region of the eye's optics [14]. Wade and Fitzke adapted a SLO to image a 2.5 x 2.5 degree field near the fovea [15]. They showed images of photoreceptors, which were only apparent after extensive image processing of the raw images [16].

The limits to microscopic imaging in the human eye are the monochromatic aberrations, which are variable in the population and are present in significant proportions through the fifth aberration order [17]. The AOSLO described in this paper uses an AO system to compensate the aberrations of any individual.

2. Methods

The AOSLO Instrument

A schematic of the AOSLO is shown on Fig. 1. The AOSLO occupies about a 1.5 x 1 m area on an optical table. The AOSLO comprises six main components, light delivery, wavefront sensing, wavefront compensation, raster scanning, light detection and frame grabbing.

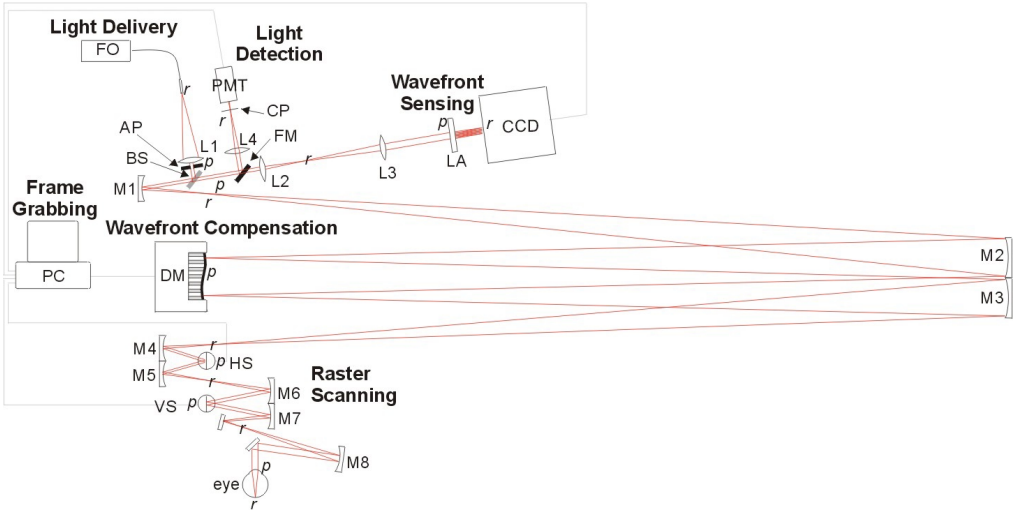

Fig. 1. The adaptive optics scanning laser ophthalmoscope. The six main components are labeled. Lenses are labeled L# and mirrors M#. Retinal and pupil conjugate points are labeled *r* and *p* through the optical path. FO: fiber optic light source, AP: artificial pupil, BS: beamsplitter, DM deformable mirror, HS: horizontal scanner (16kHz), VS: vertical scanner (30 Hz), LA: lenslet array, FM: flipping mirror, CP: confocal pinhole, PMT: photomultiplier tube.

Light Delivery: The light originates from a diode laser and is coupled into a single-mode optical fiber. The tip of the fiber provides a point source, which is collimated by a 100 mm achromatic lens. An aperture placed after the system sets the entrance pupil diameter. The entrance pupil is relayed by mirror telescopes to the deformable mirror, the horizontal scanner, the vertical scanner and finally to the eye. Mirrors are used throughout the double pass path of the instrument to keep the instrument compact, to limit chromatic dispersion, and to avoid back reflections. The drawback of using mirrors is that astigmatism and other aberrations are induced when they are used off axis. To overcome these aberrations, we allowed for a cylindrical correction to be placed at the spectacle plane of the eye and then used optical design software (ZEMAX, Focus Software, Tucson, AZ) to minimize the remaining high-order system aberrations through optimal placement of the mirrors. In the design, we were able to keep the system aberrations diffraction-limited over an imaging field of up to 4 X 4 degrees using off-the-shelf spherical reflecting mirrors [18]. Light scanning and AO correction are done in planes that are conjugate to the entrance pupil plane, which is the pivot point for the raster scanning.

#1011 - $15.00 US Received March 28, 2002; Revised April 24, 2002

Wavefront Sensing: The wave aberration is measured with the same light that is used to form the image. This is possible because, although the light is being scanned in a raster on the retina, the light is descanned on the return path, which renders the beam stationary [19]. Thus, the Shack-Hartmann wavefront sensor sees the light from the retina as though it were coming from a single spot, which makes an aberration measurement possible. This method has several advantages. First, the scanning uses the method of Hofer et al. in which scanning on the retina is employed to remove speckle from the short-exposure retinal images [19]. This is important because the light source in the AOSLO is highly coherent. A second advantage is that the average aberration is measured over the entire field of view of the system. This ensures more uniformity in the correction over the field that is being imaged. For small fields, measuring average aberrations is not expected to generate a large benefit since the eye is isoplanatic over at least one degree [20]. The final advantage is that the wavefront sensing and the imaging use the same light path and light source, which reduces non-common path errors and eliminates non-common aberrations between the wave aberration and imaging light due to chromatic effects. The actual wavefront sensor is a Shack-Hartmann type employing a square lenslet array. Each lenslet aperture is 0.4 mm square and the lenslet focal length is 24 mm. The focused spots are imaged onto a digital CCD camera. The wave aberrations are fit to a 10^{th} order Zernike polynomial.

Wavefront Compensation: A 37-channel deformable mirror (Xinetics, Andover, MA) is placed in the path conjugate to the entrance pupil of the eye. By placing the DM in the stationary part of the optical path (before the raster scanning) the size of the mirrors required for relaying the light through the system is minimized. Minimizing the mirror sizes allowed for smaller reflection angles, which reduced the inherent aberrations of the system. The size of the deformable mirror surface is 46 mm, which made it necessary to magnify the pupil. This magnification is the main reason for the large size of the device. Aberrations are corrected on both the ingoing and outgoing light paths. This is important because in a confocal SLO, optical quality is governed by aberrations in both directions [21, 22]. On the ingoing path, the aberrations are corrected to focus the light to a compact spot on the retina. On the outgoing path, correcting aberrations allow the diffusely reflected light from the eye to be refocused to a compact spot at the confocal pinhole. The mirror shape to correct the aberrations is driven from the wavefront sensing arm of the instrument. The system is run with a LabView (National Instruments, Austin, TX) interface and currently runs in a low bandwidth closed loop.

Raster Scanning: The beam is scanned on the retina with a resonant scanner – galvanometric scanner combination (Electro-Optics Products Corp, Flushing Meadows, NY). The resonant scanner scans the beam horizontally at 16 kHz in a sinusoidal pattern. The galvanometric scanner is coupled to the resonant scanner and operates in a sawtooth pattern at $1/525^{th}$ of the horizontal scan frequency. This configuration provides 525 lines per frame at about 30 frames per second. Both scanners are placed optically conjugate to the entrance pupil. This ensures that there is no movement of the scanning beam at its pivot point. The amplitude of the scan can be adjusted in the current instrument to adjust the field size from 3 X 3 to 1 X 1 degrees (for a 7 mm pupil). The resonant scanner provides the master timing for the instrument. Analog outputs from the scanner unit are converted to digital *hsync* and *vsync* signals that define the frames for the frame grabbing board

Light Detection: The light from the retina is descanned and is focused onto a confocal pinhole. In the detection arm (3.5 mm exit beam, 100 mm focal length collector lens), the ideal pinhole diameter is about 20 μm [23], but to increase throughput we used a pinhole diameter of 80 μm. The light passing through the pinhole is detected with a GaAs photomultiplier tube (Hamamatsu, Japan). After current to voltage conversion and amplification the signal is fed to the analog input of the frame grabbing board.

Frame Grabbing: Three inputs are provided to the frame grabbing board (GenesisLC, Matrox, Montreal, Canada); *hsync*, *vsync* and signal. Between each *hsync* signal the mirror goes through one full cycle of the horizontal scan. In the current implementation, the frame grabber only digitizes pixels while the scanning beam is going in the forward

#1011 - $15.00 US Received March 28, 2002; Revised April 24, 2002

direction. All 512 pixels are acquired during the central 80% of the extent of the horizontal sweep, which is the most linear part of the forward scan. Nonetheless, in the raw images, there is a non-linear horizontal magnification of the field because the sampling frequency remains constant while the mirror speed changes across the scan. All the images shown in this article have been corrected for this sinusoidal distortion. Images were acquired and stored uncompressed in a digital format. The length of the live video sequences that we could store was limited only by computer hard-disk space.

Imaging Protocol

Patients used a dental impression mount affixed to an X-Y-Z translation stage to set and maintain eye alignment during the wavefront correction and imaging. The retinal location of wavefront correction and imaging was controlled by having the subject view a fixation target. Wavefront correction and imaging was done through a 7 mm pupil. A drop of 1% tropicamide was instilled prior to imaging to dilate the pupil and minimize accommodative fluctuations. The imaging sequence began with wavefront sensing and correction. Imaging was initiated once the aberrations were reduced to a minimum. Whenever the images appeared to degrade, or if the subject sat out of the instrument for a period, we updated the aberration correction.

3. Results

Wavefront Correction

To date, we have collected images on the eyes of 5 individuals ranging in age from 22-35. The RMS wavefront error after AO compensation ranged from 0.09 to 0.15 μm over a 7 mm pupil.

Imaging

*Adaptive Optics On/Off***:** Correcting the ocular aberrations provides a dual benefit when using a small confocal pinhole. The first benefit is that more light is focused though the confocal pinhole, which reduces photon noise. We quantified the improvement by recording the light power transmitted through the confocal pinhole with the AO system turned off and on. Switching the AO *off* to *on* reduced the RMS wavefront error in an eye from 0.55 to 0.15 μm, and the light power through the confocal pinhole increased from 12 to 31 pW. The expected benefit for smaller pinholes is even greater [18]. Fig. 2 shows images of the same section of retina taken during a single image sequence where the AO system was turned off and on.

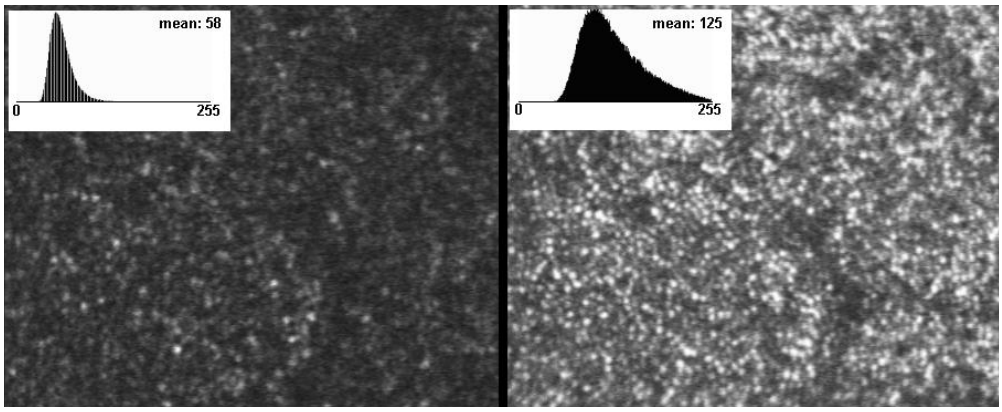

Fig. 2. The two figures show the same area of retina taken with and without aberration correction with AO. In this case, the RMS wavefront error was reduced from 0.55 to 0.10 μm. The insets show the histograms of gray scales in the image.

Axial Sectioning: The reduction in aberrations allows for true axial sectioning of the retina. Fig. 3 shows three layers of a section of retina 4.5 degrees superior to the fovea. The sections reveal the surface of the nerve fiber layer, the blood vessel that is passing through the nerve

#1011 - $15.00 US Received March 28, 2002; Revised April 24, 2002

fiber layer and the underlying photoreceptors. The image sequence spans about 300 μm of axial depth in the retina.

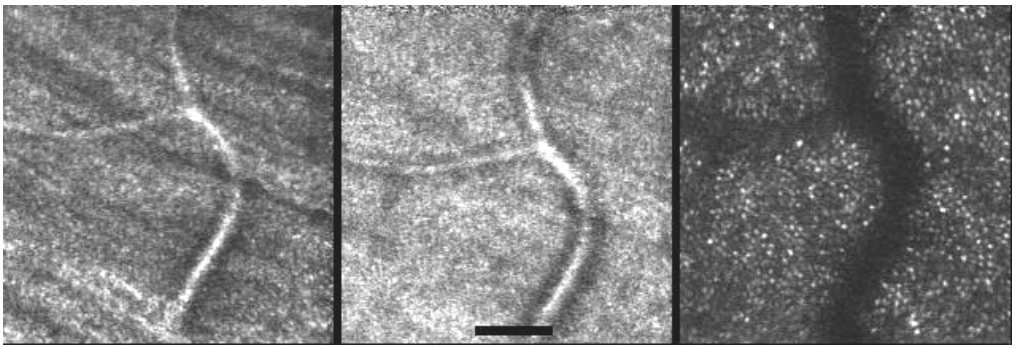

Fig. 3. Axial sectioning. These images are from a location 4.5 degrees in the superior retina. In the left image, the focal plane is at the surface of the nerve fibers. The central image shows a slightly deeper optical section where less nerve fiber structure is seen but the blood vessel is in focus. The right image shows the image when the focal plane is at the level of the photoreceptors, which are about 300 μm deeper than the left image. The blood vessel appears dark because scattered light from its surface is blocked by the confocal pinhole. Scale bar is 100 micrometers.

Dynamic Imaging and Blood Flow: Real-time, high-resolution imaging in the AOSLO permits visualization of the flow of single blood cells in the smallest retinal capillaries at the edge of the foveal avascular zone. The movie (see Fig. 4) shows a real-time image sequence where white blood cells can be seen flowing through the capillary in the lower field. The speed of the blood cells was about 1.5 mm/sec. The capillaries are close to the same plane as the photoreceptor inner segments so they are also resolved in the same movie sequence.

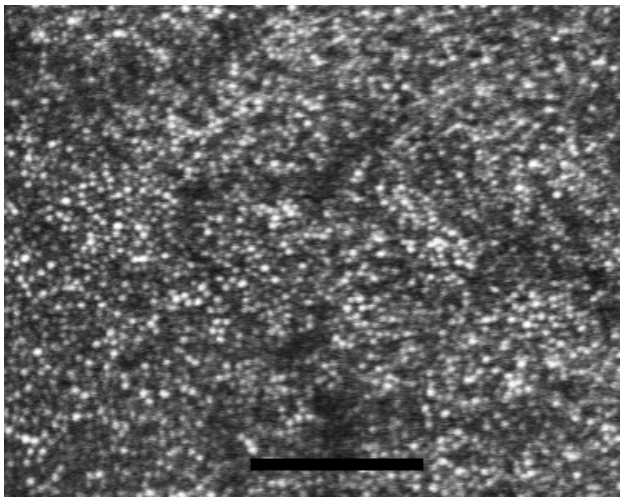

Fig. 4. (2 MB) Movie sequence (30 fps) showing the flow of white blood cells though the capillaries at the edge of the foveal avascular zone (10 MB version). The capillary is the m-shaped line in the frame. The fovea is 1 degree (450 μm) up and to the right of the center of the frame. The blood cells can be seen entering the capillary at the right side and exiting the bottom edge of the frame. The frame is a registered sum of 8 sequential frames. Some resolution of the movie is lost due to compression. Longer, uncompressed movies can be found at our website [24]: www.opt.uh.edu/research/aroorda/aoslo.htm. Scale bar is 100 microns.

#1011 - $15.00 US Received March 28, 2002; Revised April 24, 2002

Photoreceptors: To date, cone photoreceptors have been resolved at retinal locations from 0.5 to 4 degrees from the fovea. Fig. 5 shows photoreceptor spacing measured in a single subject at eight retinal locations.

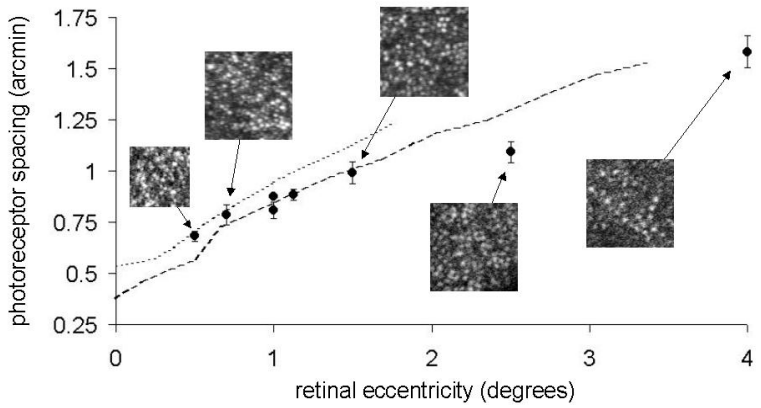

Figure 5. Change in photoreceptor spacing with eccentricity. The circle symbols show the cone photoreceptor spacing as a function of eccentricity from the fovea. The long-dashed line shows anatomical data from Curcio et al. 1990 and the short-dashed line show psychophysical estimations of cone spacing from Williams [25]. Our cone spacing estimates were made by measuring the average radius of Yellot's ring [26] from the power spectrum of the images.

4. Discussion

AOSLO vs. Conventional SLO

SLO has improved contrast and offers the added feature of axial resolution compared to conventional ophthalmoscopy [3]. However, achieving the ultimate imaging potential of the SLO is hampered by the aberrations of the eye. In the AOSLO, reducing aberrations allows the numerical aperture to be maximized, increasing light collection, and improving both lateral and axial resolution. Preliminary estimates of the resolution, which we have yet to quantify, are about 2.5 μm lateral and better than 100 μm axial. Thus, the volume resolution element in the AOSLO is reduced by more than one order of magnitude over conventional SLOs, which have a typical resolution of 5 μm lateral and 300 μm axial.

AOSLO vs. Flood-Illumination AO Ophthalmoscopy

The AOSLO has several important advantages over conventional flood-illumination imaging with AO. First, the AOSLO is real-time, operating at a frame rate of 30 Hz, which is sufficient to visualize blood flow in the retinal capillaries. This ability to image the retina in real-time also provides the operator immediate feedback on image quality and image location, which will be useful in clinical settings where efficiency in collecting data is very important. Second, flood-illuminated imaging does not allow for axial resolution. Therefore, even if AO is used, features in the best focal plane are imaged, but their contrast is reduced by out-of-focus light form the other scattering layers. The AOSLO uses a confocal aperture for axial sectioning and so only light from near the plane of best focus gets imaged. This has the dual effect of giving images higher contrast and allowing axial sectioning.

5. Conclusion

The adaptive optics scanning laser ophthalmoscope has demonstrated lateral resolution that is comparable to that obtained with flood-illuminated AO ophthalmoscope. In addition, it images the retina in real-time, it has improved contrast and adds a new dimension to AO-imaging by pushing axial resolution to a level where it is possible to do true optical sectioning of living human retina.

#1011 - $15.00 US Received March 28, 2002; Revised April 24, 2002

Acknowledgements

This work was funded by a NIH/NEI grant EY13299-01 to AR and also by the National Science Foundation Science and Technology Center for Adaptive Optics, managed by the University of California at Santa Cruz under cooperative agreement #AST-9876783.

#1011 - $15.00 US Received March 28, 2002; Revised April 24, 2002